Published in Journal of Biomechanical Engineering (Tr. ASME) vol. 134 (2012) pp: 061006-1-8

Research Article

Measurement of Multi-segment Foot Joint Angles During Gait Using a Wearable System

Hossein Rouhani[1], Julien Favre[1], Xavier Crevoisier[2], Kamiar Aminian[1]

[1] Ecole Polytechnique Fédérale de Lausanne (EPFL), Laboratory of Movement Analysis and Measurement,

Address: EPFL-STI-LMAM, Station 11, CH-1015 Lausanne, Switzerland

(hossein.rouhani@epfl.ch; julien.favre@epfl.ch; kamiar.aminian@epfl.ch)

[2] Centre Hospitalier Universitaire Vaudois and University of Lausanne (CHUV), Department of Orthopaedic Surgery and Traumatology,

Address: Avenue Pierre-Decker 4, CH-1011 Lausanne, Switzerland (xavier.crevoisier@chuv.ch)

Keywords: Inertial Sensors, Long-term Gait Analysis, Multi-segment Foot, Joint Angle, Strap-down Integration.

Corresponding Author: **Hossein Rouhani**

Address: EPFL-STI- LMAM, ELH 137/ Station 11, CH-1015 Lausanne, Switzerland

Email: hossein.rouhani@epfl.ch , Phone: +41 21 693 5675, Fax: +41 21 693 6915

Abstract

Usually, the measurement of multi-segment foot and ankle complex kinematics is done with stationary motion capture devices, which are limited to use in a gait laboratory. This study aimed to propose and validate a wearable system to measure the foot and ankle complex joint angles during gait in daily conditions, and then to investigate its suitability for clinical evaluations.

The foot and ankle complex consisted of four segments (shank, hindfoot, forefoot, and toes), with an inertial measurement unit (3D gyroscopes and 3D accelerometers) attached to each segment. The angles between the four segments were calculated in the sagittal, coronal, and transverse planes using a new algorithm combining strap-down integration and detection of low-acceleration instants. To validate the joint angles measured by the wearable system, three subjects walked on a treadmill for five minutes at three different speeds. A camera-based stationary system that used a cluster of markers on each segment was used as a reference. To test the suitability of the system for clinical evaluation, the joint angle ranges were compared between a group of ten healthy subjects and a group of twelve patients with ankle osteoarthritis, during two 50-m walking trials where the wearable system was attached to each subject.

On average, over all joints and walking speeds, the RMS differences and correlation coefficient between the angular curves obtained using the wearable system and the stationary system were 1° and 0.93, respectively. Moreover, this system was able to detect significant alteration of foot and ankle function between the group of patients with ankle osteoarthritis and the group of healthy controls.

In conclusion, this wearable system was accurate and suitable for clinical evaluation when used to measure the multi-segment foot and ankle complex kinematics during long-distance walks in daily life conditions.

1. Introduction

Kinematic assessment of the foot and ankle complex using multi-segment models requires measurements of subtle movements among foot bones. Although motion capture devices have been used for 3D body movement analysis for over 30 years, only with recent generations of more accurate devices has kinematic assessment of the foot and ankle complex using multi-segment models become feasible. This new capability is now fully used by the biomechanics community, and multi-segment foot models provided very valuable results [1-4]. However, to date, multi-segment segment models have only been used with stationary motion capture systems inside gait laboratories, so only a few consecutive gait cycles can be recorded in a limited and controlled environment using this technology. Thus, it is difficult to guarantee that the subjects walk as naturally as during their daily activities [5]. Moreover, parameters such as the variability of gait, which is a useful tool for evaluating the outcome of pathologies and clinical treatments, can only be analyzed during long-distance trials [6-7]. Wearable systems comprising inertial measurement units (IMU), including gyroscopes, accelerometers, and/or magnetometers, attached to body segments were developed to measure joint angles during daily activity and over long periods of time [8-9], but there is a lack of such a system for the monitoring of multi-segment foot and ankle kinematics.

Like stationary systems, wearable systems require two steps to measure the joint angles. First, a sensor-to-segment calibration (commonly referred as anatomical calibration) should be performed to achieve clinically meaningful and repeatable kinematic data [10]. This procedure consists of "mathematically" aligning the axes of the IMU's frame to the axes of the segment's bone-embedded anatomical frame (BAF). With stationary systems (e.g., optoelectronic motion capture systems), the calibration procedures are generally based on position measurements. However, these procedures are not appropriate for wearable systems because these devices cannot measure position accurately. While sensor-to-segment calibration procedures compatible with IMUs were recently proposed [11-14], none of these methods considered a multi-segment foot model, nor were they tested using data from subjects with lower limb pathologies. The second step consists of measuring the orientation of the BAFs during gait. The main challenge for body segment orientation measurement using IMUs is the cumulative error (drift), caused by the integration of the sensor outputs. Various algorithms were suggested to combine the information obtained by the gyroscopes, accelerometers, and/or magnetometers to reduce the drift error [15-17], and were then successfully used to calculate the 3D hip, knee, and ankle joint angles during gait [14]. Some authors also developed algorithms to measure the foot position and gait parameters using IMUs attached to the foot [18], [19], [20]. Despite these contributions to gait analysis, the monitoring of the 3D joint angles for a multi-segment foot and ankle complex model, which involves different ranges and patterns of motion than the hip and knee joints, has not yet been achieved using an IMU-based system. Moreover, these previous studies did not include any validation for long-distance gait (several tens of meters).

This study therefore proposes a wearable system to measure the 3D joint angles of the foot and ankle complex using a multi-segment model during long-distance gait. This system, consisting of four IMUs, was validated against a stationary system (reference) during five-minute walks at various speeds. Finally, the suitability of this wearable system for clinical evaluations outside a laboratory was assessed by comparing a group of patients with ankle osteoarthritis to a group of healthy controls.

2. Materials and methods

2.1. Wearable system

2.1.1 Hardware

The wearable system (Physilog, BioAGM, CH) used in this study consisted of four IMUs (each one including a 3D accelerometer and a 3D gyroscope) and two miniature data-loggers embedded in a belt. In order to ensure that the system could be used anywhere, magnetometers were not considered because the magnetic field can be distorted close to the floor [21]. Based on our previous work [22], the foot and ankle complex was decomposed into four segments: shank, hindfoot, forefoot, and toes. An IMU was affixed to each segment using medical tape (Figure 1). For calibration and validation purposes, a plate with four reflective markers was added to each IMU (Figure 1). Signals were recorded at 200 Hz.

2.1.2. Sensor-to-segment calibration

For virtual alignment of the IMU's technical frame (TF) to the corresponding segment's BAF, a mixed approach was used: first, the orientation of the BAFs and TFs during a calibration phase was determined using an auxiliary system; second, gait was monitored

using only the wearable system [14]. This approach allows the use of previously validated calibration procedures based on position measurements. To this end, before the walking trials, the subjects were asked to stand still while an examiner palpated anatomical landmarks on their foot and measured their position using a pointer, which was part of the auxiliary system. For this study, the same stationary system, consisting of seven infra-red cameras (VICON, Oxford, UK), was used as the auxiliary system for the calibration and the reference system for the validation. The same BAF definition (Table 1) [23] was used for the four segments, and was selected because it is frequently used. However, the method presented in this study can be adapted for any BAF definition. Based on the position of the anatomical landmarks, the rotation matrices corresponding to the orientation of the BAFs with respect to the laboratory frame (LF), R_{BAF}^{LF}, were calculated. Similarly, the orientation of the IMU's TF with respect to LF, R_{TF}^{LF}, was calculated using the markers attached to each IMU. For each segment, the rotation matrix between the BAF and the corresponding TF, R_{TF}^{BAF}, was obtained using (Eq. 1).

$$R_{TF}^{BAF} = \left(R_{BAF}^{LF}\right)^{-1} . R_{TF}^{LF} \tag{1}$$

Then, the angular velocity and acceleration measured by the IMU ($\vec{\omega}^{TF}$, $\vec{S}^{TF}$) were expressed in the segment's BAF using Eqs. 2 and 3.

$$\vec{\omega}^{BAF}(t) = \left[\omega_x(t)\,,\,\omega_y(t)\,,\,\omega_z(t)\right]^T = R_{TF}^{BAF} . \vec{\omega}^{TF}(t) \tag{2}$$

$$\vec{S}^{BAF}(t) = \left[S_x(t)\,,\,S_y(t)\,,\,S_z(t)\right]^T = R_{TF}^{BAF} . \vec{S}^{TF}(t) \tag{3}$$

where *t* represents the time sample.

2.1.3. Segment orientation calculation

In order to allow long-distance gait measurement without drift, a specific algorithm using two constraints of the stance phase was designed. This algorithm required three steps: 1) identification of the gait phases, 2) calculation of an initial orientation for the segments during a motionless instant of mid-stance based on an inclination (angle with the vertical axis) and an azimuth (direction in the horizontal plane) estimate, 3) calculation of the segment orientation during stance by forward and backward strap-down integration.

Step 1: The heel-strike, toe-off, and stance phase time (between heel-strike and toe-off) were detected for each cycle based on the shank angular velocity [24].

Step 2: For each segment, an initial orientation was needed for the strap-down integration of step 3. The initial orientation was determined during a quasi-static period where the inclination could be estimated directly from the accelerometer [15,25]. In fact, when the segment acceleration is small, the accelerometer's output is approximately equal to the gravity (Eq. 4).

$$\vec{S}^{BAF} = \vec{g}^{BAF} - \vec{a}^{BAF} \cong \vec{g}^{BAF} \quad (4)$$

where $\vec{S}$ is the accelerometer output, $\vec{g}$ is the gravity, and $\vec{a}$ is the segment acceleration, all expressed in the segment BAF.

In this study, the time of initial orientation (t_0) was fixed at 50% of stance phase for the toes and at 40% of stance phase for the other segments. The gait of three controls walking at different speeds for several minutes (Section 2.3.1) showed that at these percentages of stance phase, the difference between the norm of the accelerometer output ($\vec{S}$) and $\vec{g}$ (9.81 m.s^{-2}) was less than 0.5 m.s^{-2} on average and always less than 1.0 m.s^{-2}. This choice of

t_0 agrees with a recent study [26] that reported zero-velocity instants of foot motion during gait.

In the horizontal plane, the azimuth was systematically set to zero at t_0, since the IMUs were already aligned with the BAF and because only walking in a straight line was considered in this study.

Therefore, $R_{BAF}^{LF}(t_0)$, the initial orientation of each BAF ($[\vec{x},\vec{y},\vec{z}]$) with respect to LF ($[\vec{X},\vec{Y},\vec{Z}]$), was calculated as follows. First, the $\vec{Y}$ axis (vertically upwards) was calculated relative to the BAF assuming $\vec{S}(t_0)$ equal to gravity (Eq. 5).

$$\vec{Y}^{BAF}(t_0) = R_{LF}^{BAF}(t_0).\vec{Y}^{LF}(t_0) = -\frac{\vec{S}(t_0)}{\left\|\vec{S}(t_0)\right\|} \tag{5}$$

Then, since the azimuth is defined as being equal to zero at t_0, $\vec{x}$ is in the plane of $\vec{X}$ and $\vec{Y}$. Therefore, $\vec{Z}$ is perpendicular to the plane of $\vec{x}$ and $\vec{Y}$, and can be calculated using (Eq. 6).

$$\vec{Z}^{BAF}(t_0) = R_{LF}^{BAF}(t_0).\vec{Z}^{LF}(t_0) = \frac{\vec{x}^{BAF}(t_0)\times\vec{Y}^{BAF}(t_0)}{\left\|\vec{x}^{BAF}(t_0)\times\vec{Y}^{BAF}(t_0)\right\|} = \frac{[1,0,0]^T\times\vec{Y}^{BAF}(t_0)}{\left\|[1,0,0]^T\times\vec{Y}^{BAF}(t_0)\right\|} \tag{6}$$

Since the axes of LF are orthogonal, $\vec{X}$ is calculated as the cross product of $\vec{Y}$ and $\vec{Z}$ (Eq. 7).

$$\vec{X}^{BAF}(t_0) = R_{LF}^{BAF}(t_0).\vec{X}^{LF}(t_0) = \vec{Y}^{BAF}(t_0)\times\vec{Z}^{BAF}(t_0) \tag{7}$$

Finally, $R_{BAF}^{LF}(t_0)$ is obtained by matrix inversion (Eq. 8).

$$R_{BAF}^{LF}(t_0) = \left[\vec{X}^{BAF}(t_0) \quad , \quad \vec{Y}^{BAF}(t_0) \quad , \quad \vec{Z}^{BAF}(t_0)\right]^{-1} \tag{8}$$

Step 3: The orientation of the segment at any time of stance (t) was incrementally calculated based on the orientation ($R_{BAF}^{LF}(t-1)$) and angular velocity ($\vec{\omega}(t-1)$) during the previous time sample (t-*1*) using strap-down integration (Eq. 9).

$$R_{BAF}^{LF}(t) = R_{BAF}^{LF}(t-1).Exp_m\left(t_s.\begin{bmatrix} 0 & -\omega_z(t-1) & \omega_y(t-1) \\ \omega_z(t-1) & 0 & -\omega_x(t-1) \\ -\omega_y(t-1) & \omega_x(t-1) & 0 \end{bmatrix}\right) \quad (9)$$

where t_s is the sampling period and Exp_m is the exponential function for matrices as defined in [27]. For each segment, the initial orientation ($R_{BAF}^{LF}(t_0)$) was calculated according to step 2. Then, using forward (from t_0 to toe-off) and backward (from t_0 to heel-strike) strap-down integration, the orientation was calculated during the complete stance phase of the gait cycle. In this study, the joint angles were only considered during the stance phase of gait, due to their clinical significance during this phase.

2.1.4. Joint angle calculation

The joint angles between the proximal and distal segments were calculated from $R_{BAF}^{LF}\big|_{proximal}$ and $R_{BAF}^{LF}\big|_{distal}$ based on the joint coordinate system formulation [28]. According to [29], dorsiflexion, inversion, and internal rotation were defined as positive angles. Three joints were considered for the foot and ankle complex: shank~hindfoot (SH-HF), hindfoot~forefoot (HF-FF), and forefoot~toes (FF-TO). Shank~forefoot (SH-FF) was also considered since the ankle model used in many clinical publications is closer to SH-FF than to SH-HF [30-31]. Because the difference in morphology among subjects could offset the angular curves, for each trial, the mean angle was subtracted from the angular curve to obtain relative angles [32].

2.2. Stationary system

A stationary optoelectronic motion capture system (VICON, UK) consisting of seven cameras was used as reference in this study because this is the kind of system most

frequently used to measure multi-segment foot kinematics [1-4]. To compare the angles obtained by the wearable system and the stationary system, a lightweight plate (below 10 g) with four reflective markers was firmly attached to each IMU (Figure 1) during the treadmill walking trials (the plates were not used during the corridor walks). Since the inertia of these custom-made plastic plates was small, their effects on the measurements were minimal. The BAF and TF definitions and the calculation of the joint angles were exactly the same as previously described for the wearable system. The reference system was operated at 200Hz, synchronously with the wearable system.

2.3. System assessment

2.3.1. Comparison to a stationary system

For the first part of the study, which aimed to assess the differences between the wearable system and the stationary system, three healthy controls (female: 26 years, 52 kg, 168 cm; male: 27 years, 68 kg, 171 cm; male: 27 years, 76 kg, 180 cm) were enrolled. Once equipped with the systems detailed in Sections 2.1 and 2.2, they walked on a treadmill at three speeds (2, 3.5, and 5 km/h) for five minutes per speed. Before each walking trial, the subject was asked to stand still for 15 seconds. This posture was used to determine the initial offsets of the gyroscope signals, which were then removed during the following walking trial. The relative angular curves were calculated for both the wearable system and the stationary system during the stance phase of all gait cycles. The differences between these angles were then quantified by the root mean square (RMS) differences and by the correlation coefficients (R). Additionally, due to their clinical significance, the ranges of motion (ROM) of the four joints were also compared between the wearable system and the stationary system.

2.3.2 Clinical application

Twelve patients with unilateral ankle osteoarthritis (9 male, 60±15 years old, 170±6 cm, 81±18 kg) and ten healthy controls (3 male, 61±13 years old, 166±9 cm, 67±10 kg) took part in this phase of the study. Patients reported Foot Function Index (FFI) of 48±17 and American Orthopaedic Foot and Ankle Society (AOFAS) score for the ankle-hindfoot of 47±14. Participants were equipped with the wearable system described in Section 2.1 and then completed two trials of a 50-m walk in a hospital corridor. Based on literature [30-31], it was hypothesized that patients with ankle osteoarthritis would have reduced motion at the ankle and midtalar joints. Therefore, the average ROM of SH-HF, HF-FF, and SH-FF joints in the sagittal, coronal, and transverse planes were calculated for each participant considering all the cycles of both trials. Then, the patients and healthy control groups were compared using the Wilcoxon rank-sum test. The Ethics committee approved this study and subjects gave their informed consent prior to testing.

3. Results

The joint angles obtained using the wearable system were very similar to the angles obtained using the stationary system (reference) in terms of amplitude and pattern, as is illustrated for the intermediate walking speed in Figure 2. The differences between the joint angle curves measured by the wearable system and the stationary system are quantified as RMS differences and correlation coefficients in Figure 3. The mean RMS differences (computed over all the gait cycles of all subjects) for the foot joint angles along each axis of rotation were below 1.2°, 1.4°, and 2.0° for the slow, medium, and fast walking speeds, respectively. Moreover, the overall average of these mean RMS differences across

all speeds, rotation axes, and foot joints was 1.0°. The mean correlation coefficients (over all the gait cycles of all subjects) between the angular curves measured by the wearable system and the angular curves measured by the stationary system were higher than 0.82 for all speeds, rotation axes, and joints, and the overall average of these mean correlation coefficients was 0.93 (Figure 3).

Over all the gait cycles of all subjects, the mean differences between the ROMs measured by the wearable system and the stationary system had amplitudes below 4° for all foot joints, rotation axes, and speeds. Furthermore, the mean amplitude of these differences between the ROMs measured by the wearable and stationary systems over all speeds, joints, and rotation axes was 1.4°. Box-plots of the differences in ROM and the absolute ROM as measured by the stationary system, which can be used to estimate the relative ROM differences between the two systems, are presented in Figure 4.

For most of the joint angles (78%), the ROMs were significantly different (p-value<0.05) between the patient and the healthy control groups (Table 2), with smaller ROMs in the patient group. For SH-FF, the ROMs were statistically different in the three anatomical planes, and for SH-HF and HF-FF, the sagittal and transverse ROMs were statistically different.

4. Discussion

This study, for the first time, showed that the 3D joint angles of the foot and ankle complex described using a multi-segment model can be measured over long-distance gait using body-worn IMUs. This system provides the means to conduct measurements in natural conditions and to test other variables, such as variability, coordination, or fatigue. The

calculation of the 3D angles was done on a gait cycle basis and therefore did not depend on the previous gait cycles, which allowed precise measurement of any duration (five-minute trials in this study). Finally, the suitability of this system for clinical evaluation was demonstrated by comparing the gait of two groups of individuals with different ankle conditions.

When compared to the stationary system, the angular curves obtained by the proposed wearable system resulted in mean RMS differences between 0.5° and 2.0°, and correlation coefficients between 0.82 and 0.99 for all foot joints and speeds (Figure 3). In addition, the amplitude of the mean ROM differences was below 4° with an average of 1.4° over all foot joints and speeds. It should be noted that the systematic ROM differences (presented as median values in the box-plots of Figure 4) affect the results of all subjects equivalently and should not influence the comparison between subject groups in clinical evaluations. As shown in Figures 3 and 4, the difference between the joint angles measured by the two systems generally increased with walking speed. This observation can be explained by the fact that faster walking speed results in higher angular velocity of the foot segments, and according to Eq. 9, the error in the calculated segment orientation is directly dependent on the magnitude of the angular velocity and its error in the measurement. The differences between the two systems were, in general, smaller in the sagittal plane than in the other planes (Figures 3 and 4). In fact, the calculation of $R(t_0)$ in Eqs. 5-8 used a measure for the inclination of the segment in the sagittal plane (Eq. 5) and a constraint for the azimuth angle. Therefore, the error of $R(t_0)$ was smaller in the in the sagittal plane than in the other planes, which resulted in larger differences between the joint angles obtained by the two systems in the coronal and transverse planes than in the sagittal plane.

The angles obtained by the wearable system were only slightly different from the angles obtained by the traditional stationary system. In order to investigate whether the proposed wearable system can be used for clinical applications despite these subtle differences, the new system was used to compare the foot kinematics of healthy controls and patients with ankle osteoarthritis. As is usually done in the literature[20,33-34], joint ROMs were compared and as hypothesized, most of the joint angles were significantly smaller for the patients compared to the healthy controls. These results agreed with previous studies [30-31] and showed that the wearable system was sensitive enough to distinguish between patients with reduced ankle and midtalar motion and healthy controls.

To the authors' knowledge, this was the first time that two biomechanical constraints of gait, (i.e., the quasi-static condition of the foot and ankle complex during foot-flat and the consistent horizontal alignment among segments while walking in a straight line) were used for monitoring the 3D joint angles of a multi-segment foot over long-distance gait. Compared to previous wearable systems, the results of the present study showed smaller or comparable differences between the stationary (reference) and the wearable systems; Favre et al. [9] reported mean RMS difference of 1.6° for the knee angles and Sabatini [17] reported RMS difference between 1.0° and 2.9°. Incorporating the biomechanical constraints of gait allowed our method to perform the strap-down integration cycle by cycle. As shown in this study, this technique was efficient at suppressing integration drift and allowed accurate measurement of joint angles over long periods of time.

Compared to standard in-lab motion capture techniques (e.g., cameras or fluoroscopy), the proposed wearable system allows for the measurement of foot movement in any environment and over long-distances. The light weight (only 375 g) and minimal

encumbrance of this system should allow more natural kinematics to be measured [5]. Moreover, this system can capture a high number of consecutive gait cycles, allowing for the analysis of cycle-to-cycle variations, which have been shown to be potentially important parameters for clinical evaluations [6,35]. The system presented in this study used a mixed approach [14] because this combines the advantages of stationary and wearable motion capture systems. It is important to repeat that with this approach, the stationary device is only used for a standard and reliable sensor-to-segment (anatomical) calibration step prior to the field measurement. In the future, reliable calibration procedures suitable for a multi-segment foot and ankle complex model based only on IMU signals are expected, and will eliminate the need for an auxiliary system.

This study proposes a method to calculate the 3D multi-segment foot joint angles during walking on level ground in a straight line for any duration. To keep the system and its operation as simple as possible, the proposed method assumed that the azimuth angle is known at specific time points during foot-flat, and used this assumption to determine the relative orientation of each segment with respect to the others. While relative orientations are sufficient to calculate joint angles, if the absolute orientation of any segment or the foot progression angle are of interest, the method can be extended to measure the actual azimuth angles, for example by adding magnetometers.

5. Conclusion

This study described a wearable system based on four inertial measurement units including 3D gyroscopes and 3D accelerometers to measure the joint angles of the foot and ankle complex during walking. This system used a multi-segment model to describe the

rotations between the shank, hindfoot, forefoot, and toes in the sagittal, coronal, and transverse planes. Compared to a widely used stationary system, this new wearable system reported good agreement in terms of joint angles pattern and amplitude. Moreover, this system was able to detect slight alteration of foot and ankle function between a group of patients with ankle osteoarthritis and a group of healthy controls. Therefore, this wearable system, which has been shown to be efficient in analyzing long-distance walking under natural conditions, can be a valuable tool to study a variety of foot pathologies and treatments.

Conflict of interest

There is no conflict of interest.

Acknowledgement

The work was supported by "Fonds National Suisse de la Recherche Scientifique", grant No. 3200B0-120422/1. The authors would like to thank Prof. Brigitte Jolles for her collaboration, Dr. Mehdi Gholamrezaee for his advice about statistical analyses, and Mr. Pascal Morel and Mr. Jean Gramiger for their assistance during the measurement.

References

1. Eslami M, Begon M, Farahpour N, Allard P (2007) Forefoot-rearfoot coupling patterns and tibial internal rotation during stance phase of barefoot versus shod running. Clinical Biomechanics 22(1): 74-80

2. Leardini A, Benedetti MG, Berti L, Bettinelli D, Nativo R, Giannini S (2007) Rear-foot, mid-foot and fore-foot motion during the stance phase of gait. Gait and Posture 25(3): 453-462

3. Canseco K, Long J, Marks R, Khazzam M, Harris G (2009) Quantitative motion analysis in patients with hallux rigidus before and after cheilectomy. Journal of Orthopaedic Research 27(1): 128-134

4. Baker R, Robb J (2006) Foot models for clinical gait analysis. Gait and Posture 23(4): 399-400

5. Bussmann JBJ, Veltink PH, Koelma F, Van Lummel RC, Stam HJ (1995) Ambulatory monitoring of mobility-related activities: The initial phase of the development of an activity monitor. European Journal of Physical Medicine and Rehabilitation 5(1): 2-7

6. Najafi B, Helbostad JL, Moe-Nilssen R, Zijlstra W, Aminian K (2009) Does walking strategy in older people change as a function of walking distance? Gait and Posture 29(2): 261-266

7. Lindemann U, Najafi B, Zijlstra W, Hauer K, Muche R, Becker C, Aminian K (2008) Distance to achieve steady state walking speed in frail elderly persons. Gait and Posture 27(1): 91-96

8. Dejnabadi H, Jolles BM, Aminian K (2005) A new approach to accurate measurement of uniaxial joint angles based on a combination of accelerometers and gyroscopes. IEEE Transactions on Biomedical Engineering 52(8): 1478-1484

9. Favre J, Jolles BM, Aissaoui R, Aminian K (2008) Ambulatory measurement of 3D knee joint angle. Journal of Biomechanics 41(5): 1029-1035

10. Cappozzo A, Della Croce U, Leardini A, Chiari L (2005) Human movement analysis using stereophotogrammetry: Part 1: theoretical background. Gait and Posture 21(2): 186-196

11. Picerno P, Cereatti A, Cappozzo A (2008) Joint kinematics estimate using wearable inertial and magnetic sensing modules. Gait and Posture 28(4): 588-595

12. O'Donovan KJ, Kamnik R, O'Keeffe DT, Lyons GM (2007) An inertial and magnetic sensor based technique for joint angle measurement. Journal of Biomechanics 40(12): 2604-2611

13. Favre J, Aissaoui R, Jolles BM, de Guise JA, Aminian K (2009) Functional calibration procedure for 3D knee joint angle description using inertial sensors. Journal of Biomechanics 42(14): 2330-2335

14. Favre J, Crevoisier X, Jolles BM, Aminian K (2010) Evaluation of a mixed approach combining stationary and wearable systems to monitor gait over long distance. Journal of Biomechanics 43(11): 2196-2202

15. Favre J, Jolles BM, Siegrist O, Aminian K (2006) Quaternion-based fusion of gyroscopes and accelerometers to improve 3D angle measurement. Electronics Letters 42(11): 612-614

16. Roetenberg D, Luinge HJ, Baten CTM, Veltink PH (2005) Compensation of magnetic disturbances improves inertial and magnetic sensing of human body segment orientation. IEEE Transactions on Neural Systems and Rehabilitation Engineering 13(3): 395-405

17. Sabatini AM (2006) Quaternion-based extended Kalman filter for determining orientation by inertial and magnetic sensing. IEEE Transactions on Biomedical Engineering 53(7): 1346-1356

18. Sabatini AM, Martelloni C, Scapellato S, Cavallo F (2005) Assessment of walking features from foot inertial sensing. IEEE Transactions on Biomedical Engineering 52(3): 486-494

19. Schepers HM, Koopman HFJM, Veltink PH (2007) Ambulatory assessment of ankle and foot dynamics. IEEE Transactions on Biomedical Engineering 54(5): 895-902

20. Mariani B, Hoskovec C, Rochat S, Büla C, Penders J, Aminian K (2010) 3D gait assessment in young and elderly subjects using foot-worn inertial sensors. Journal of Biomechanics 43(15): 2999-3006

21. de Vries WHK, Veeger HEJ, Baten CTM, van der Helm FCT (2009) Magnetic distortion in motion labs, implications for validating inertial magnetic sensors. Gait and Posture 29(4): 535-541

22. Rouhani H, Favre J, Crevoisier X, Jolles BM, Aminian K (2011) Segmentation of foot and ankle complex based on kinematic criteria. Computer Methods in Biomechanics and Biomedical Engineering 14(9): 773-781

23. Cappozzo A, Catani F, Della Croce U, Leardini A (1995) Position and orientation in space of bones during movement: Anatomical frame definition and determination. Clinical Biomechanics 10(4): 171-178

24. Salarian A, Russmann H, Vingerhoets FJ, Dehollain C, Blanc Y, Burkhard PR, Aminian K (2004) Gait assessment in Parkinson's disease: toward an ambulatory system for long-term monitoring. IEEE Transactions on Biomedical Engineering 51(8): 1434-43

25. Dejnabadi H, Jolles BM, Casanova E, Fua P, Aminian K (2006) Estimation and visualization of sagittal kinematics of lower limbs orientation using body-fixed sensors. IEEE Transactions on Biomedical Engineering 53(7): 1385-1393

26. Peruzzi A, Della Croce U, Cereatti A (2011) Estimation of stride length in level walking using an inertial measurement unit attached to the foot: A validation of the zero velocity assumption during stance. Journal of Biomechanics 44(10): 1991-1994

27. Higham NJ (2009) The scaling and squaring method for the matrix exponential revisited. SIAM Review 51(4): 747-764

28. Grood ES, Suntay WJ (1983) A joint coordinate system for the clinical description of three-dimensional motions: Application to the knee. Journal of Biomechanical Engineering 105(2): 136-144

29. Wu G, Siegler S, Allard P, Kirtley C, Leardini A, Rosenbaum D, Whittle M, D'Lima DD, Cristofolini L, Witte H, Schmid O, Stokes I (2002) ISB recommendation on definitions of joint coordinate system of various joints for the reporting of human joint motion - Part I: Ankle, hip, and spine. Journal of Biomechanics 35(4): 543-548

30. Valderrabano V, Nigg BM, von Tscharner V, Stefanyshyn DJ, Goepfert B, Hintermann B (2007) Gait analysis in ankle osteoarthritis and total ankle replacement. Clinical Biomechanics 22(8): 894-904

31. Ingrosso S, Benedetti MG, Leardini A, Casanelli S, Sforza T, Giannini S (2009) GAIT analysis in patients operated with a novel total ankle prosthesis. Gait and Posture 30(2): 132-137

32. Kadaba MP, Ramakrishnan HK, Wootten ME, Gainey J, Gorton G, Cochran GVB (1989) Repeatability of kinematic, kinetic, and electromyographic data in normal adult gait. Journal of Orthopaedic Research 7(6): 849-860

33. Bae J, Kong K, Byl N, Tomizuka M (2011) A mobile gait monitoring system for abnormal gait diagnosis and rehabilitation: A pilot study for parkinson disease patients. Journal of Biomechanical Engineering 133(4):

34. Rouhani H, Favre J, Crevoisier X, Aminian K (2011) Ambulatory Measurement of Ankle Kinetics for Clinical Applications. Journal of Biomechanics 44(15): 2712-2718

35. Dubost V, Annweiler C, Aminian K, Najafi B, Herrmann FR, Beauchet O (2008) Stride-to-stride variability while enumerating animal names among healthy young adults: result of stride velocity or effect of attention-demanding task? Gait and Posture 27(1): 138-43

Tables

Table 1. Anatomical landmarks used to construct the bone-embedded anatomical frame (BAF) and definition of the BAF for the three foot segments and for the shank.

Table 2. ROM (in degree) for the SH-HF, HF-FF, and SH-FF joints during the over-ground walks for the healthy and ankle osteoarthritis groups presented as median (inter-quartile range). In case of significant difference (p-value<0.05) between the two groups, the p-value is reported.

Figures

Figure 1. a) Portable data-logger, IMU, and IMU equipped with a rigid plate and four reflective markers, b) IMUs attached on shank and foot segments: Shank (Tibia and Fibula), Hindfoot (Calcaneus and Talus), Forefoot (Navicular, Cuboid, Cuneiform, Metatarsals) and Toes (Phalanges). The rigid plates were used only for calibration and validation purpose.

Figure 2. Relative joint angle curves during stance time of 3.5 km/h walks for SH-HF, HF-FF, FF-TO, and SH-FF in three anatomical planes: dorsiflexion-plantarflexion (sagittal), inversion-eversion (coronal), and internal rotation-external rotation (transverse). Grey curves correspond to the wearable system and black curves correspond to stationary system. Results are presented as mean angle curve (solid) and mean±std (dashed) over all the gait cycles of the three subjects.

Figure 3. RMS differences (a,b,c) and correlation coefficients (d,e,f) between the joint angles measured by the wearable system and the stationary system. The box-plots report the median, 1st and 3rd quartiles, and the minimum and maximum whiskers for all stance phases of the three subjects collected during five minutes of walking. Results are presented for the sagittal (S), coronal (C), and transverse (T) planes.

Figure 4. ROM differences (a,b,c) between the wearable system and the stationary system presented as box-plots (median, 1st and 3rd quartiles, and the minimum and maximum whiskers) for all stance phases of the three subjects collected during five minutes of walking. ROMs measured by the stationary system are also presented (d,e,f) to express the relative ROM differences between the two systems. Results are presented for the sagittal (S), coronal (C), and transverse (T) planes .

Tables

Table 1.

Anatomical landmarks of foot	
CA	The great tuberosity of the calcaneus
FM	The apex of head of the 1st metatarsal
SM	The apex of head of the 2nd metatarsal
VM	The apex of head of the 5th metatarsal
BAF for all segments	
X-axis	On the intersection of the following planes with positive direction in anterior direction: - Quasi-transverse plane: Defined by CA, FM, and VM - Quasi-sagittal plane: Orthogonal to quasi-sagittal plane, going through CA and SM
Z-axis	Perpendicular to the quasi-sagittal plane with positive direction from left to right
Y-axis	Completing the right handed frame

Table 2.

Joint	Rotation plane	Healthy	Ankle Osteoarthritis	Comparison
Shank-Hindfoot	**Sagittal**	14.6(0.6)	11.0(2.9)	**p=0.001**
	Coronal	7.9(2.1)	6.8(4.3)	
	Transverse	8.9(8.9)	6.7(3.2)	**p=0.019**
Hindfoot-Forefoot	**Sagittal**	13.8(6.6)	10.1(2.7)	**p=0.001**
	Coronal	4.5(3.9)	5.8(2.4)	
	Transverse	5.2(3.6)	3.3(2.2)	**p=0.032**
Shank-Forefoot	**Sagittal**	25.0(8.9)	18.2(7.6)	**p<0.001**
	Coronal	9.2(4.2)	6.4(2.8)	**p=0.013**
	Transverse	14.3(7.2)	6.9(3.2)	**p=0.003**

Figures

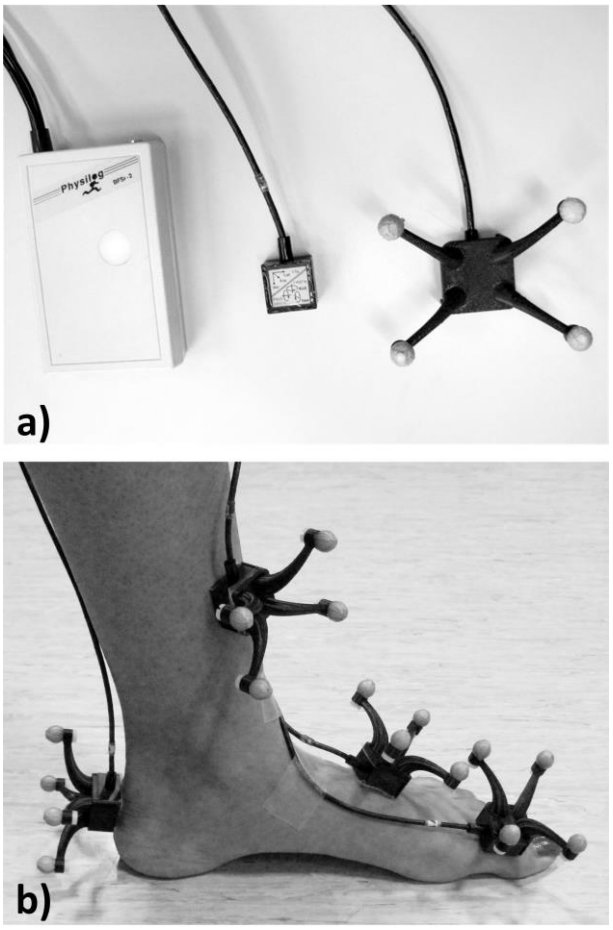

Figure 1.

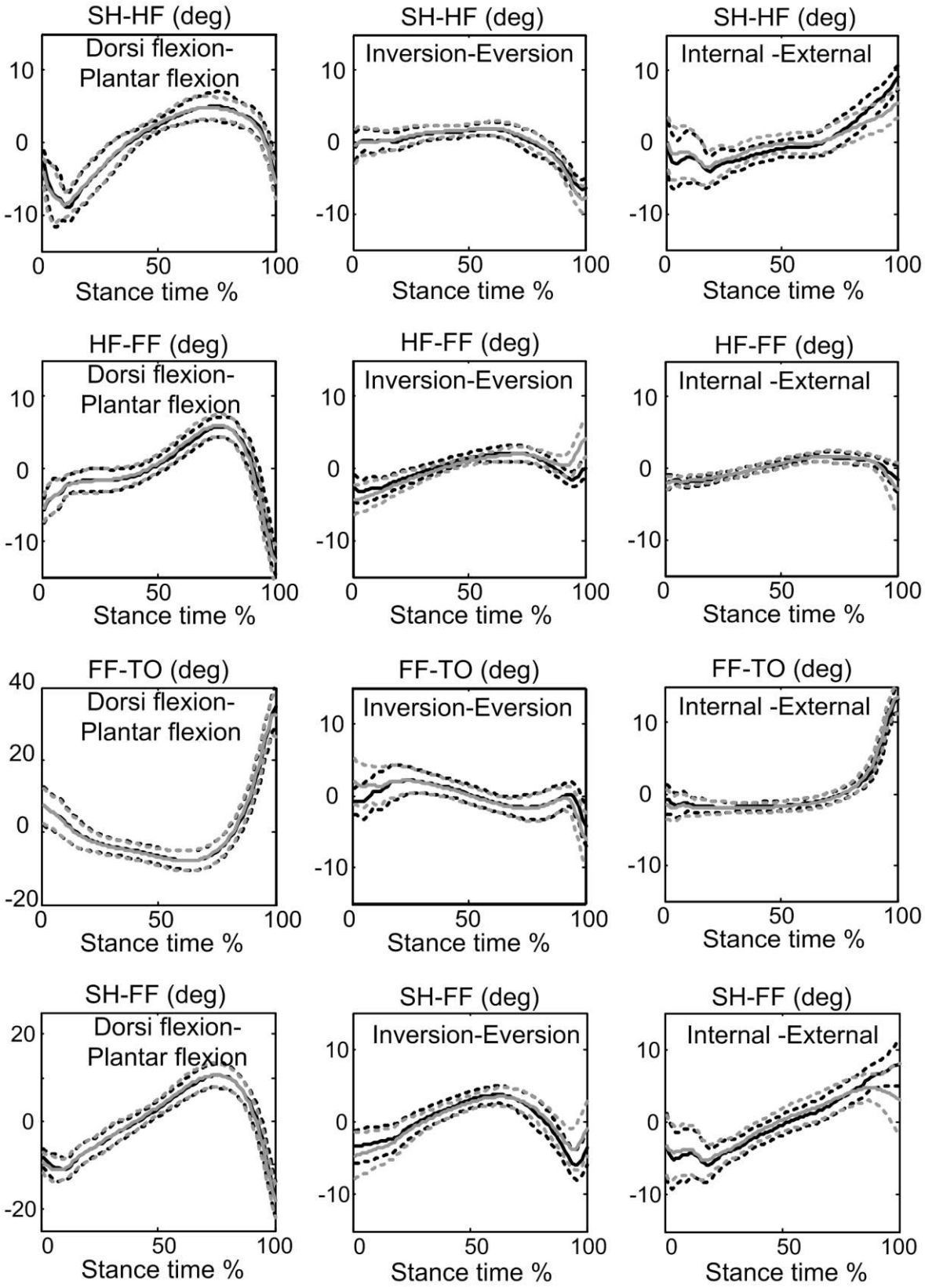
SH-HF (deg)
Dorsi flexion-
Plantar flexion
SH-HF (deg)
Inversion-Eversion
SH-HF (deg)
Internal -External
HF-FF (deg)
Dorsi flexion-
Plantar flexion
HF-FF (deg)
Inversion-Eversion
HF-FF (deg)
Internal -External
FF-TO (deg)
Dorsi flexion-
Plantar flexion
FF-TO (deg)
Inversion-Eversion
FF-TO (deg)
Internal -External
SH-FF (deg)
Dorsi flexion-
Plantar flexion
SH-FF (deg)
Inversion-Eversion
SH-FF (deg)
Internal -External
Stance time %

Figure 2.

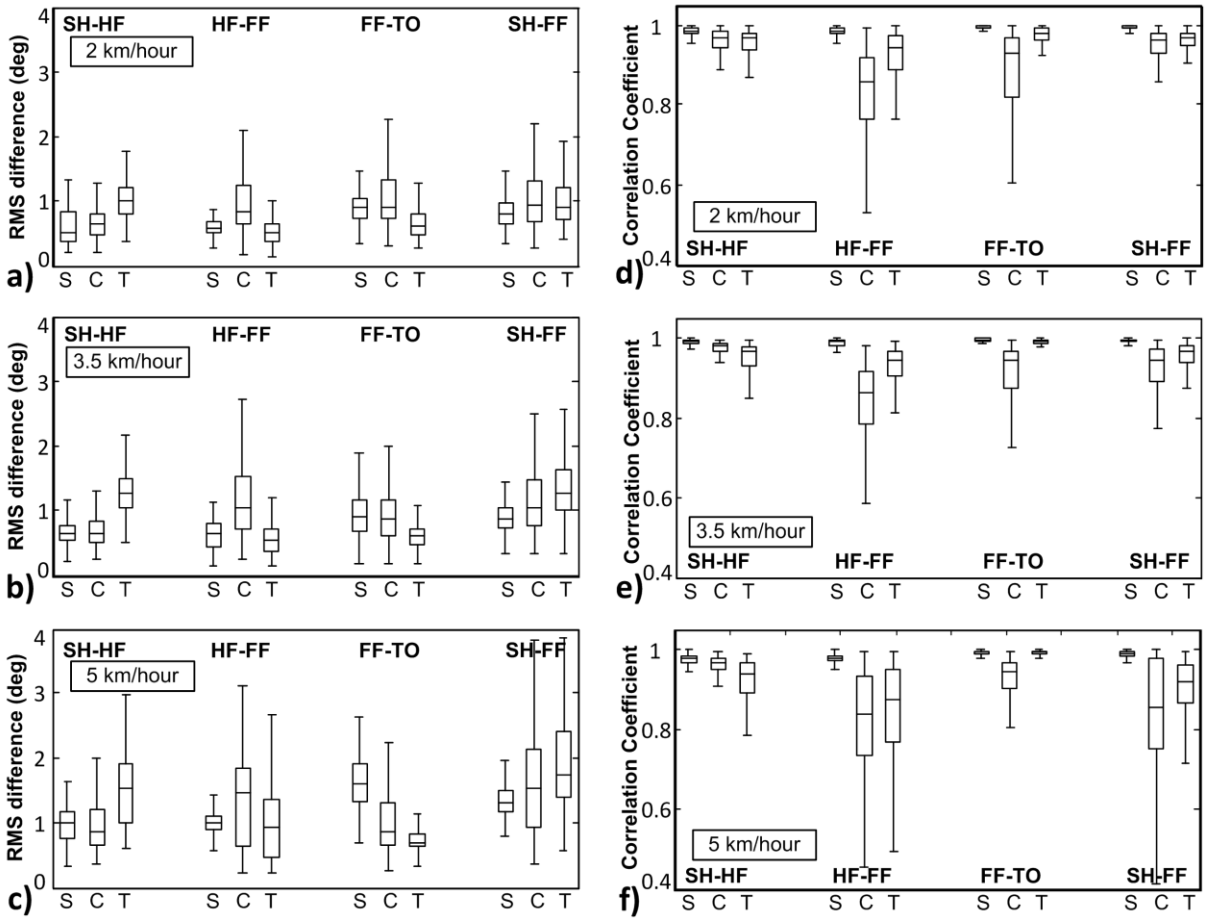
a)
b)
c)
d)
e)
f)
RMS difference (deg)
Correlation Coefficient
SH-HF
HF-FF
FF-TO
SH-FF
S C T
2 km/hour
3.5 km/hour
5 km/hour

Figure 3.

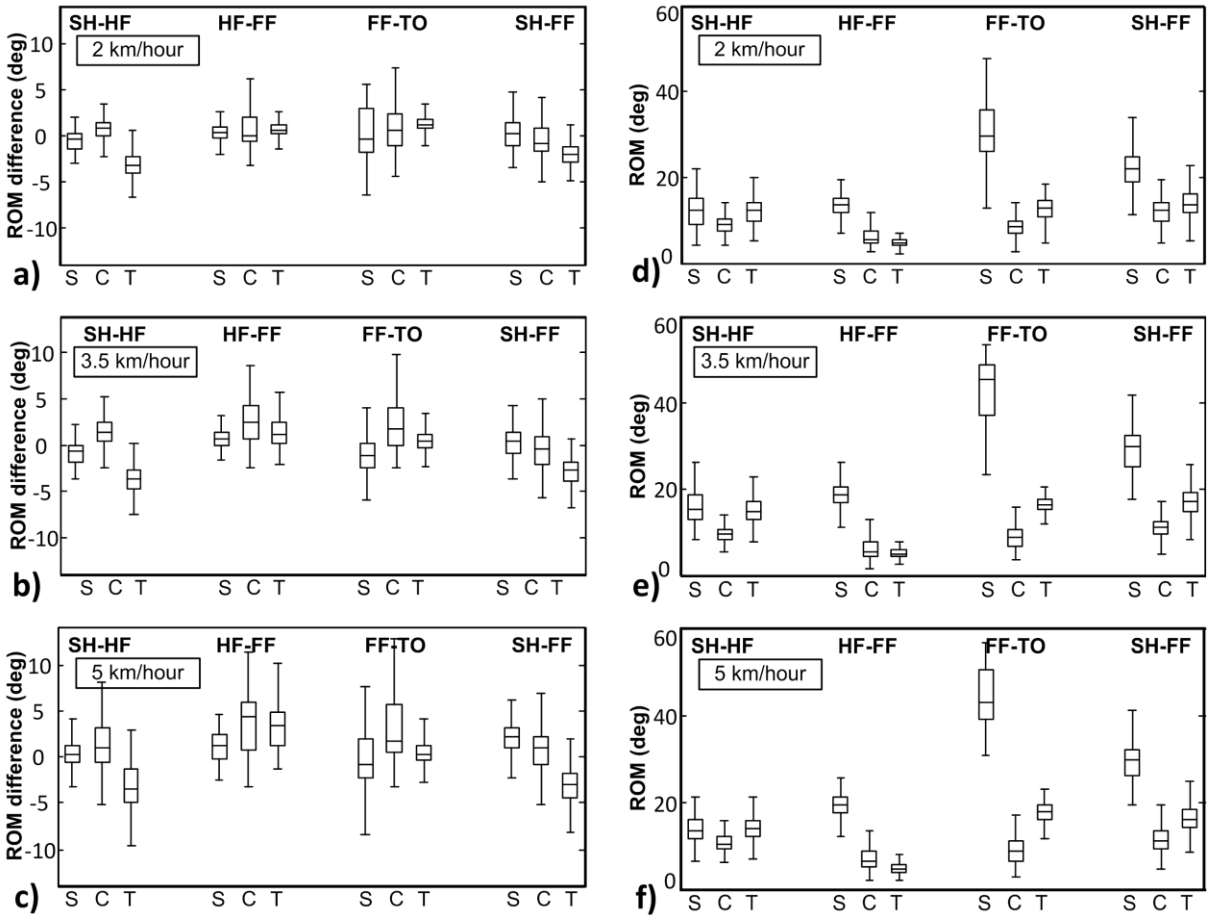
SH-HF
HF-FF
FF-TO
SH-FF
2 km/hour
3.5 km/hour
5 km/hour
ROM difference (deg)
ROM (deg)
S C T
a)
b)
c)
d)
e)
f)

Figure 4.